Monitoring human information processing via intelligent data analysis of EEG recordings

Arthur Flexer[1] and Herbert Bauer[2]

[1] The Austrian Research Institute for Artificial Intelligence
Schottengasse 3, A-1010 Vienna, Austria
arthur@ai.univie.ac.at
[2] Department of Psychology, University of Vienna
Liebiggasse 5, A-1010 Vienna, Austria

Abstract. Human information processing can be monitored by analysing cognitive evoked potentials (EP) measurable in the electro encephalogram (EEG) during cognitive activities. In technical terms, both visualization of high dimensional sequential data and unsupervised discovery of patterns within this multivariate set of real valued time series is needed. Our approach towards visualization is to discretize the sequences via vector quantization and to perform a Sammon mapping of the codebook. Instead of having to conduct a time-consuming search for common subsequences in the set of multivariate sequential data, a multiple sequence alignment procedure can be applied to the set of one-dimensional discrete time series. The methods are described in detail and results obtained for spatial and verbal information processing are shown to be statistically valid, to yield an improvement in terms of noise attenuation and to be well in line with psychophysiological literature.

1 Introduction

Psychophysiological studies use the method of cognitive evoked potentials measurable in the encephalogram (EEG) during cognitive activities to monitor physiological correlates of human information processing. EEG is a non-invasive method to record electric brain potentials from the human scalp via a set of electrodes. We speak of cognitive evoked potentials (EPs) when the EEG is recorded from a test subject who is solving a cognitive task during recording. An EP is defined as the combination of the brain electric activity that occurs in association with the eliciting event and 'noise', which is brain activity not related to the event together with inference from non-neural sources. Since the noise contained in EPs is significantly stronger than the signal, the common approach is to compute an average across several EPs recorded under equal conditions to improve the signal-to-noise ratio. The average $\hat{s}(t)$ over the sample of N EPs is used to estimate the underlying signal $s(t)$:

$$\hat{s}(t) = \frac{1}{N}\sum_{i=1}^{N} x_i(t) = s(t) + \frac{1}{N}\sum_{i=1}^{N} n_i(t); \quad i = 1, 2, \ldots N; \quad 0 \leq t < T \qquad (1)$$

where $x_i(t)$ is the ith recorded EP, $s(t)$ the underlying signal, $n_i(t)$ the noise associated with the ith EP, and T the duration over which each EP is recorded. The crucial assumption behind averaging is that the evoked signal $s(t)$ is the same for each recorded EP $x_i(t)$. Whereas this is true for simpler sensoric or motoric events, cognitive activities do not elicit one specific EP waveform time locked to the onset of the recording. Only subsequences of the whole EPs that do not occur at fixed time after the onset of the recording can be expected to be due to the cognitive task.

Our approach towards the analysis of cognitive evoked potentials (EP) combines several intelligent data analysis methods (see Fig. 1) to tackle these problems. Since each EP is measured via a number of electrodes it is a multidimensional time series. After appropriate filtering, we visualize this high dimensional sequential set of data by replacing the sequence of the original vectors by a sequence of prototypical codebook vectors obtained from a clustering procedure. Additionally, a dimensionality reduction technique is applied to obtain an ordered one-dimensional representation of the high dimensional codebook vectors that allows for the depiction of the original sequence as a one-dimensional time series. Searching for common subsequences in the vast set of real valued multivariate sequential data is computationally prohibitive. Instead we can use the set of univariate discrete time series, the trajectories across codebook vectors, and apply a multiple sequence alignment procedure for comparison of sequences. Finally, we are able to compute an alternative selective average across the obtained subsequences.

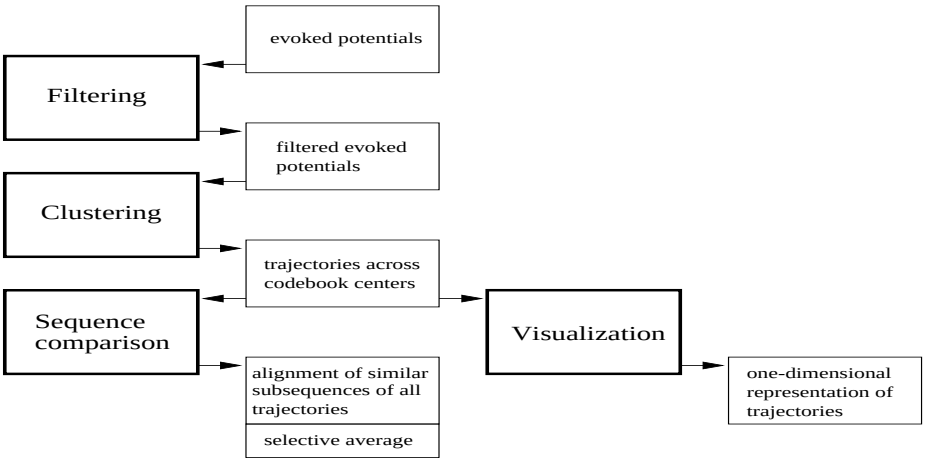

Fig. 1. Flow diagram of the spatio-temporal clustering approach.

Especially the analysis of the temporal structure of cognitive EPs is a largely unsolved problem in psychophysiology. Classical methods like [15, 10, 9] and [14] are designed for univariate time series of simpler motoric or sensoric EPs only.

They usually assume that the recorded univariate signal is the same for all EPs during the whole duration of the recording but allow variable latencies of the common waveform. Therefore they cannot really cope with the harder problem of analysing cognitive EPs. Existing data mining approaches to processing of sequential patterns are not applicable to our problem for the following reasons: Template based approaches require a query pattern or frequent episode [8] to be defined before the search is started which is not possible for cognitive EPs since only very vague knowledge about the subsequences to be discovered exists. Template based approaches are also designed for univariate or symbolic sequences only. The same holds for specialized approaches given e.g. in [6] and [2] which have the additional problem of being hard to link to a model of cognitive EPs.

Our work is structured in the following way: First we describe the EP data sets and then all applied methods (clustering, visualization, sequence comparison) are presented in detail. Statistical significance is ensured via comparison with results obtained for artificial data sets, the gain in noise attenuation relative to common averaging is quantified and the results for spatial and verbal information processing are shown to be well in line with literature. All computer experiments have been done within a rigorous statistical framework using appropriate statistical tests.

2 The data

The data stems from 10 good and 8 poor female spatializers who were subjected to both a spatial imagination and a verbal task. The complete data base of EP recordings is therefore divided into four groups: 319 EPs spatial/good, 167 EPs spatial/poor, 399 EPs verbal/good, 270 verbal/poor. After appropriate preprocessing (essentially limiting the signals to frequencies below $8Hz$ and eliminating the DC-like trend by subtracting a linear fit), each EP trial consists of 2125 samples, each being a 22 dimensional real valued vector. One complete 22-channel EP trial (duration is 8.5 seconds) is depicted in Fig. 2(a). The discretization step described in Sec. 3 will make the analysis of this vast data set computationally tractable.

3 Clustering and visualization

The EP time series are vector quantized together by using all the EP vectors at all the sample points as input vectors to a clustering algorithm disregarding their ordering in time. Then the sequence of the original vectors x is replaced by the sequence of the prototypical codebook vectors $\hat{x}$. There is a double benefit of this step: it is part of the visualization scheme and the sequences of $\hat{x}$ serve as input to the sequence comparison procedure.

K-means clustering (see e.g. [3, p.201]) is used for vector quantization using the sum of squared differences $d(x, \hat{x}) = \sum_{i=0}^{k-1} \mid x_i - \hat{x}_i \mid^2$ as measure of distance, where both x and $\hat{x}$ are of dimension k. Since observation of the sum of distances

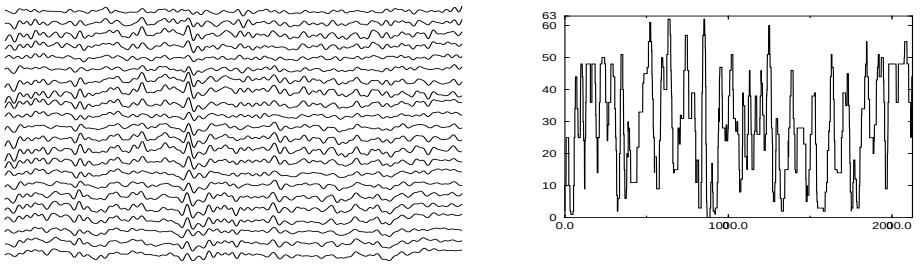

(a) (b)

Fig. 2. (a) Example of a complete 8.5 second 22-channel EP recording. (b) The corresponding trajectory across codebook vectors depicted as ordered codebook numbers (y-axis) as a function of time (x-axis).

$d(x, \hat{x})$ with growing size of codebooks did not indicate an optimal codebook size, we pragmatically decided to use 64 codebook vectors which is sufficient to preserve all important features in the sequence of codebook vectors. "Important" features are positive and negative topographical peaks and their development in time. The high number of different discrete symbols (64 codebook vectors) did not allow for a more principled information theoretic approach to obtain an optimal codebook size. Instead of a set of 22-dimensional time series, we now have sequences of discrete symbols, where each symbol is drawn from the alphabet of the 64 codebook vectors $\hat{x}$. For the 64 codebook vectors, we calculated a 64×64 distance matrix D_C.

The sequences of codebook vectors can be visualized in a graph where the x-axis stands for time and the y-axis for the number of the codebook vector. Since in the course of time, the trajectory moves only between codebook vectors that are close to each other in the 22 dimensional vector space, this neighbourhood should also be reflected by an appropriate ordering of the numbers of the codebook vectors. Such an ordered numbering results in smooth curves of the time vs. codebook number graphs and enables visual inspection of similarities between trajectories. We obtain such an ordered numbering by first performing a Sammon mapping [12] of the 22-dimensional codebook vectors to one output dimension and by then renumbering the codebook vectors according to a trivially achieved ordering of their one-dimensional representation. This combined technique of K-means clustering plus Sammon mapping of the codebook is described in [4] and an application to the analysis of EP data in [5]. An example for a trajectory across an ordered set of codebook vectors is given in Fig. 2(b). Note that the ordering of the numbers of the codebook vectors is needed only for visualization and is not necessary for the subsequent sequence alignment.

4 Sequence comparison

We chose a so-called *fixed length subsequence* approach for comparison of the sequences made of 64 discrete symbols (corresponding to 64 codebook vectors $\hat{x}$). Given two sequences E and F of length m, all possible overlapping subsequences having a particular window length W from E are compared to all subsequences from F. For each pair of elements the score taken from the distance matrix D_C is recorded and summed up for the comparison of subsequences. The distance between two subsequences of length W from two sequences E and F is therefore:

$$D_{align}(b_e, b_f, W) = \sum_{i=0}^{W-1} d(E_{b_e+i}, F_{b_f+i}) \tag{2}$$

The indices b_e and b_f are the beginning points of the subsequences in the sequences E and F and E_{b_e+i} and F_{b_f+i} are the corresponding codebook vectors. Successive application of this pairwise method allows for the alignment of more than two sequences. Such a *fixed subsequence* approach that is explicitly designed for *multiple sequence alignment* is given by [1]. It computes a multiple alignment by iteratively comparing sequences to the multiple alignment obtained so far, keeping always just the L best subsequences as an intermediate result.

This approach to multiple sequence alignment is called *progressive alignment*. It works by constructing a succession of pairwise alignments. Initially, two sequences are chosen at random and aligned via the *fixed length subsequence* approach described above. The L best pairwise alignments (i.e. pairs of subsequences) with minimum distances D_{align} are now fixed and stored in a heap. Then a third sequence is chosen at random and aligned to all the L pairwise alignments. The L best three-way alignments are now fixed and stored in the heap. This process is iterated until all sequences have been aligned.

When a subsequence is compared to an intermediate "more"-way (let us say p-way) subsequence, the resulting score is computed as the sum of the p pairwise comparisons of the subsequences in the intermediate solution with the new subsequence that is to be aligned. The number of all such crosswise comparisons within the final overall alignment is given by $P = \sum_{i=1}^{p-1} i$. The number of all element-wise comparisons within the final overall alignment is given by WP, and its average per element, the average element-wise within alignment distance, by:

$$\bar{D}_{align} = \frac{1}{WP} \sum_{i=1}^{p-1} \sum_{j=i+1}^{p-1} D_{align}(b_i, b_j, W) \tag{3}$$

Desired is a set of beginning points b_i^{min} for which $\bar{D}_{align}$ is minimal. The b_i^{min} are the same for all $d = 22$ channels of the corresponding ith EP. To diminish the variability of the results of this stochastic algorithm (random usage of sequences during iteration), we compute five such alignments and obtain an overall alignment and overall beginning points b_i^{min5} at the points in time where the sums of the five $\bar{D}_{align}$ are minimal. The number of single element-wise comparisons to obtain one alignment is $LW(m+1-W)P$. For a given L and m, this

function is proportional to p^2, in contrast with m^p comparisons in "brute force" searching where not just the L best but all possible alignments are considered. As experiments with L equal 100, 1000 and 10000 showed, it is sufficient to keep 100 intermediate results to avoid the omission of good alignments that are weak in the first few sequences but strong in the later ones. Experiments varying the window length W from 31 to 62, 125 and 187 showed that $W = 125$ (corresponding to $500ms$ of EP) is short enough to yield alignments of satisfactory quality which are still long enough to be significant in terms of their psychophysiological interpretation. For more detail on tuning of the parameters L and W see [5].

For each channel of EP we can compute an alternative selective average $\hat{s}'(t)$ where the duration T is equal to the length of the subsequences, W, and the beginning points of the averaging are the parameters b_i^{min5}:

$$\hat{s}'(t) = \frac{1}{N} \sum_{i=1}^{N} x_i(b_i^{min5} + t); \quad 0 \leq t < W \tag{4}$$

5 Results

In a related study [5] working on a subset of our EP data we have shown the statistical significance of our approach. We verified that our procedure yields better results for real human EPs than for unstructured random input in terms of average element-wise within alignment distance $\bar{D}_{align}$ (see Equ. 3). We compared results obtained from 21 EPs of one test subject with time-shuffled EPs and artificial EPs. The latter consisted of random Gaussian sequences whose power spectrum was changed appropriately to resemble the characteristics of real EPs. A one-way analysis of variance plus additional Duncan t-Tests allowed us to rank the result for real EP as being significantly better than the result for time-shuffled EP, which is again significantly better than the result for random Gaussian EP.

To compare the gain in noise attenuation of the common average and of our selective average, the respective estimated standard deviations of the background noise, $\hat{\sigma}(t)$ and $\hat{\sigma}'(t)$, are being compared.

$$\hat{\sigma}(t) = \left[\frac{\sum_{i=1}^{N} [x_i(t) - \hat{s}(t)]^2}{N-1} \right]^{\frac{1}{2}} \tag{5}$$

$$\hat{\sigma}'(t) = \left[\frac{\sum_{i=1}^{N} \left[x_i(b_i^{min5} + t) - \hat{s}'(t)\right]^2}{N-1} \right]^{\frac{1}{2}} \tag{6}$$

Since the $\hat{\sigma}(t)$ and $\hat{\sigma}'(t)$ are given for each of the $d = 22$ channels and for the duration of $t = m$ or $t = W$ respectively, the following average estimates of the standard deviations of the background noise are being computed:

$$\hat{S} = \frac{1}{dm} \sum_{j=1}^{d} \sum_{t=0}^{m-1} \hat{\sigma}_j(t) \tag{7}$$

$$\hat{S}' = \frac{1}{dW} \sum_{j=1}^{d} \sum_{t=0}^{W-1} \hat{\sigma}'_j(t) \tag{8}$$

$\hat{S}$ is the estimate for common averaging and $\hat{S}'$ for selective averaging. An $\hat{\sigma}_j(t)$ is the $\hat{\sigma}(t)$ for channel j given by Equ. 5. An $\hat{\sigma}'_j(t)$ is the $\hat{\sigma}'(t)$ for channel j given by Equ. 6. For all EPs of good and poor spatializers doing the spatial imagination task the common average $\hat{s}$ as well as five selective averages $\hat{s}'$ have been computed. Results for good spatializers were $\hat{S} = 7.68$ vs. mean $\hat{s}' = 4.35 \pm .068$ and for poor spatializers $\hat{S} = 7.84$ vs. mean $\hat{s}' = 4.37 \pm .048$. Computing Z-values shows the differences in noise attenuation to be significant:

$$Z_{good} = |(4.35 - 7.68)/(.068/\sqrt{5})| = |-109.5| > Z_{99} = 2.58;$$

$$Z_{poor} = |(4.37 - 7.84)/(.048/\sqrt{5})| = |-161.6| > Z_{99} = 2.58.$$

The estimated expected magnitude of the noise residual is now only ≈ 0.56 times that of the respective common averages. This is a gain in noise attenuation of more than 40%.

The results of computing selective averages via beginning points b_i^{min5} for both good and poor spatializers doing the spatial imagination task are given in Fig. 3 as sequences of topographical patterns. Each topography is a spherical spline interpolation of the 22 values at a single point in time of the selective averaging window. Given are topographies at $40, 80, \cdots, 440, 480 msec$ of the window for poor spatializers (top two rows) and good spatializers (lower two rows). We can see that for both groups there is one specific dominant topographical pattern visible, albeit at changing levels of amplitude. It is a pattern of more positive amplitudes at frontal to central regions relative to more negative amplitudes at occipital to parietal regions. This common topographical pattern is generally more negative for poor spatializers.

Our results obtained via the method of selective averaging have also been analysed by a series of analyses of variance (ANOVA). In accordance with the procedure of analysis of classical averages, selective averages of EPs are computed separately for each test subject and serve as inputs to the ANOVAs. A selective average $\hat{s}'(t)$ is computed separately for a test subject by averaging across all corresponding EPs, where the starting points of the averaging are the parameters b_i^{min5} and the duration is equal to the length of the subsequences, W.

Besides factors "Task" (spatial vs. verbal), "Performance" (good vs. poor) and "Location" (electrode position) we decided to include another factor "Time" into our analyses. This factor is needed to describe the variation of the amplitude level of the selective averages within the course of time. Six evenly spaced points in time within the selective averaging window suffice to allow for a proper analysis of this temporal variation.

The first analysis of variance was computed to test for significance of the general differences between spatially and verbally evoked subsequences of topographies. The results of this Task (two repeated measures: spatial vs. verbal) $\times$

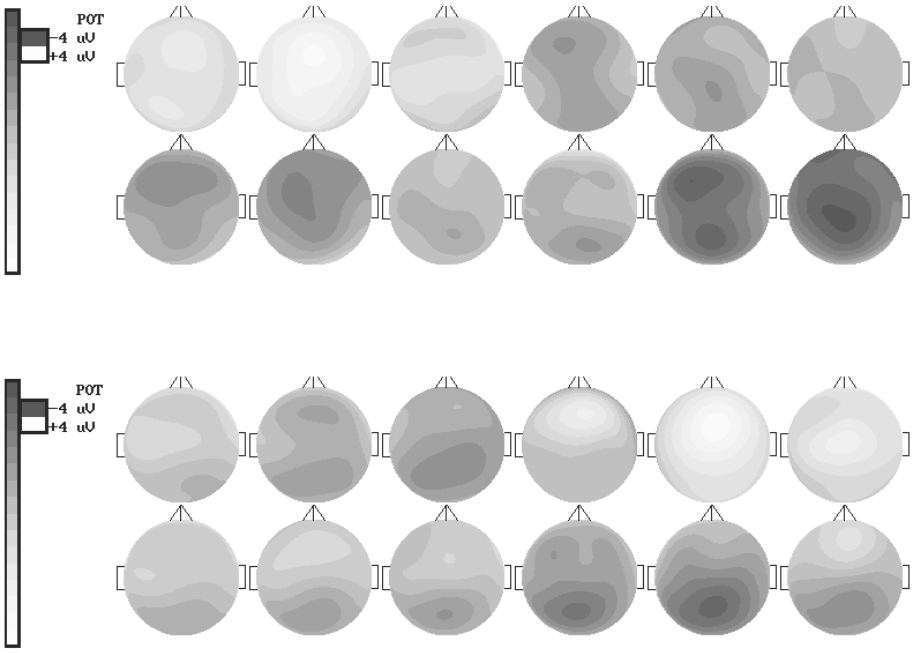

Fig. 3. Sequences of topographies for poor spatializers (top two rows) and good spatializers (lower two rows). Scale is from -4 to $+4mV$.

Table 1. ANOVA for spatial versus verbal task.

N=16 (8 spatial, 8 verbal)	Summary of all effects; Design: 1-TASK, 2-TIME, 3-LOCATION							
Effect	df Effect	df Error	ϵ_{GG}	$df_{adj.}$ Effect	$df_{adj.}$ Error	F	p-level	$p_{adj.}$
1	1	15	1.000	1.000	15.000	33.853	.000	.000
2	5	75	.497	2.485	37.280	6.425	.000	.002
3	21	315	.100	2.109	31.639	8.949	.000	.001
1 × 2	5	75	.539	2.695	40.432	7.360	.000	.001
1 × 3	21	315	.115	2.418	36.276	1.551	.060	.223
2 × 3	105	1575	.031	3.246	48.684	13.917	.000	.000
1 × 2 × 3	105	1575	.047	4.967	74.510	13.777	.000	.000

Time (6 repeated measures: amplitudes of the EPs at $0, 100, 200, 300, 400, 500ms$ in the selective averaging window) $\times$ Location (22 repeated measures: electrode positions) ANOVA are given in Tab. 5. The sample size is $N = 16$, since only 8 persons have been subjected to both the spatial and the verbal condition. On the chosen significance level of $\alpha = 5\%$ all three main effects as well as all two-way combined effects, except the Task $\times$ Location effect,and the three-way combined effect are highly significant. All corresponding values of the probability of the null hypothesis being true are very small, $P \leq 0.001$ most of the time, which is still true for the Greenhouse-Geisser (given in column ϵ_{GG}) adjusted probabilities $p_{adj.}$. The significant difference between spatial and verbal task in terms of their cortical activity distribution is of course well in line with psychophysiological literature. The more negative amplitudes at occipital to parietal regions visible in Fig. 3 are as expected and we get the additional information that both kinds of information processing are accompanied by a series of activations and in-activations.

Table 2. ANOVA for spatial task, good versus poor performers.

N=18 (10 good, 8 poor)	Summary of all effects; Design: 1-PERFORMANCE, 2-TIME, 3-LOCATION							
Effect	df Effect	df Error	ϵ_{GG}	$df_{adj.}$ Effect	$df_{adj.}$ Error	F	p-level	$p_{adj.}$
1	1	16				7.999	.012	
2	5	80	.502	2.510	40.164	8.369	.000	.000
3	21	336	.131	2.758	44.122	7.187	.000	.001
1 $\times$ 2	5	80	.502	2.510	40.164	6.432	.000	.002
1 $\times$ 3	21	336	.131	2.758	44.122	3.962	.000	.017
2 $\times$ 3	105	1680	.076	8.015	128.238	10.002	.000	.000
1 $\times$ 2 $\times$ 3	105	1680	.076	8.015	128.238	18.537	.000	.000

Taking this difference into account, data of good vs. poor spatial performers were analysed separately within task "spatial" and task "verbal". The results of these Performance (good vs. poor) $\times$ Time (6 repeated measures: amplitudes of the EPs at $0, 100, 200, 300, 400, 500ms$ in the selective averaging window) $\times$ Location (22 repeated measures: electrode positions) ANOVAs are given in Tab. 5 for spatial data and in Tab. 5 for verbal data. The sample size for the spatial data is $N = 18$, consisting of 10 good and 8 poor spatial performers. On the chosen significance level of $\alpha = 5\%$ all main and combined effects are significant, both before and after the Greenhouse-Geisser adjustment. For the verbal data, on the significance level of $\alpha = 5\%$ the main effect for the factor "Performance" is not significant, whereas most of the combined effects still are. Since the two performance levels "good" and "poor" represent extreme groups of spatial ability selected by psychological testing, they should be discriminable in their EP correlates during the spatial but not during the verbal task. This is exactly what we have found and others [13] have also reported and attributed to a higher investment of cortical effort visible as a more negative amplitude level of one similar pattern.

Table 3. ANOVA for verbal task, good versus poor performers.

N=16 (8 good, 8 poor)	Summary of all effects; Design: 1-PERFORMANCE, 2-TIME, 3-LOCATION							
Effect	df Effect	df Error	ϵ_{GG}	$df_{adj.}$ Effect	$df_{adj.}$ Error	F	p-level	$p_{adj.}$
1	1	14				0.440	.518	
2	5	70	.469	2.345	32.832	19.873	.000	.001
3	21	294	.215	4.520	63.276	105.623	.000	.000
1 × 2	5	70	.469	2.345	32.832	2.916	.316	.318
1 × 3	21	294	.215	4.520	63.276	11.949	.000	.000
2 × 3	105	1470	.072	7.611	106.559	16.102	.000	.000
1 × 2 × 3	105	1470	.072	7.611	106.559	4.045	.000	.001

6 Discussion

The analysis of cognitive evoked potentials is a largely unsolved problem in psychophysiological research. Classical methods are designed for univariate time series of simpler motoric or sensoric EPs only and can therefore not really cope with the harder problem of analysing cognitive EPs. Nevertheless they are still state of the art.

We have developed a general approach to the visualization of high dimensional sequential data and the unsupervised discovery of patterns within multivariate sets of time series data by combining several intelligent data analysis techniques in a novel way. Our method allows the analysis of cognitive evoked potentials by finding common multivariate subsequences in a set of EPs which have fixed length but variable latencies and are sufficiently similar across all EP channels. With this new kind of selective averaging it is possible to better analyse the temporal structure of the cognitive processes under investigation.

We were able to validate our approach both on a statistical basis and in terms of the psychophysiological content of the obtained results: we demonstrated statistical significance by comparison with results obtained for artificial data and by quantifying the gain in noise attenuation; we showed the plausibility of our results by comparing them to what is already known about the psychophysiology of the human brain.

Our general approach to the visualization of high dimensional sequential data and the unsupervised discovery of patterns within multivariate sets of time series data is of course not restricted to the problem presented in this work. The methods described can either be applied to multivariate real valued data by using the full approach including the transformation to sequences of discrete symbols through vector quantization plus Sammon mapping or, if already symbolic sequences are available, the fixed segment algorithm alone can be applied. Our approach is also open to using more advanced techniques of sequence comparison, like e.g. Hidden Markov Models [11].

Acknowledgements: The EEG recordings have been made by R. Gstättner, Dept. of Psychology, University of Vienna. Parts of this work were done within the BIOMED-2 BMH4-CT97-2040 project SIESTA, funded by the EC DG XII. The Austrian Research Institute for Artificial Intelligence is supported by the Austrian Federal Ministry of Science and Transport. The author was supported by a doctoral grant of the Austrian Academy of Sciences.

References

1. Bacon D.J., Anderson W.F.: Multiple Sequence Alignment, Journal of Molecular Biology, 191, 153-161, 1986.
2. Boyd S.: Detecting and Describing Patterns in Time-Varying Data Using Wavelets, in [7].
3. Duda R.O., Hart P.E.: Pattern Classification and Scene Analysis, John Wiley & Sons, N.Y., 1973.
4. Flexer A.: Limitations of Self-Organizing Maps for Vector Quantization and Multidimensional Scaling, in Mozer M.C., et al.(eds.), Advances in Neural Information Processing Systems 9, MIT Press/Bradford Books, pp.445-451, 1997.
5. Flexer A., Bauer H.: Discovery of Common Subsequences in Cognitive Evoked Potentials, in Zytkow J.M. & Quafafou M.(eds.), Principles of Data Mining and Knowledge Discovery, Second European Symposium, PKDD '98, Proceedings, Lecture Notes in Artificial Intelligence 1510, p.309-317, Springer, 1998.
6. Howe A.E., Somlo G.: Modeling Discrete Event Sequences as State Transition Diagrams, in [7].
7. Liu X., Cohen P., Berthold M.(eds.): Advances in Intelligent Data Analysis, Second International Symposium, IDA-97, Lecture Notes in Computer Science, Springer Verlag, LNCS Vol. 1280, 1997.
8. Mannila H., Toivonen H., Verkamo A.I.: Discovery of Frequent Episodes in Event Sequences, Data Mining and Knowledge Discovery, Volume 1, Issue 3, 1997.
9. McGillem C.D., Aunon J.I.: Measurements of signal components in single visually evoked brain potentials, IEEE Transactions on Biomedical Engineering, 24, 232-241, 1977.
10. Pfurtscheller G., Cooper R.: Selective averaging of the intracerebral click evoked responses in man: an improved method of measuring latencies and amplitudes, Electroencephalography and Clinical Neurophysiology, 38: 187-190, 1975.
11. Rabiner L.R., Juang B.H.: An Introduction To Hidden Markov Models, IEEE ASSP Magazine, 3(1):4-16, 1986.
12. Sammon J.W.: A Nonlinear Mapping for Data Structure Analysis, IEEE Transactions on Comp., Vol. C-18, No. 5, p.401-409, 1969.
13. Vitouch O., Bauer H., Gittler G., Leodolter M., Leodolter U.: Cortical activity of good and poor spatial test performers during spatial and verbal processing studied with Slow Potential Topography, International Journal of Psychophysiology, Volume 27, Issue 3, p.183-199, 1997.
14. Weerd J.P.C.de, Kap J.I.: A Posteriori Time-Varying Filtering of Averaged Evoked Potentials, Biological Cybernetics, 41, 223-234, 1981.
15. Woody C.D.: Characterization of an adaptive filter for the analysis of variable latency neuroelectric signals, Medical and Biological Engineering, 5, 539-553, 1967.